Fiber Length Attrition in Additive Manufacturing

June 8, 2016

Michael Chapiro

A senior project in partial fulfillment of a B.S. degree in materials engineering from California Polytechnic University of San Luis Obispo, California

Contents

List of Figures

List of Tables

Abstract

Chopped carbon fibers are used as reinforcements in thermoplastics, but the viscous shear forces that arise in melt-processing reduces the fiber length well below its critical length resulting in only moderate strength and stiffness gains compared to the neat resin. This research project aimed to experimentally determine the effect of the melt–flow portion of a single-screw-extrusion process on carbon fiber length attrition in isolation from the immediately preceding screw–plastication step that is responsible for most of the heat needed for melting. Carbon fibers with an initial length of 2 mm were stirred into 5,000 centipoise and 10,000 centipoise silicone oils at a fiber volume fraction of 10%. Each suspension was passed through a single–screw–extruder under the same conditions and the resultant fiber length distributions were compared for absolute and relative amounts of length attrition. Silicone oil suspensions of fibers were shown to be a viable method of determining the effect of the melt–phase of the extrusion process. Both samples showed similar amounts of fiber attrition. The final fiber lengths were not reduced as much as what is found in complete thermoplastic composite processing methods that include screw–plastication. Therefore, it is suggested that further research focus on how to reduce damage from screw–plastication (possibly by eliminating it) rather than on decreasing polymer viscosity in attempts to preserve fiber length.

1 Introduction

1.1 Stakeholders, purpose, and deliverables

As a non-sponsored project, I am the sole stakeholder of this project, and in accordance with Cal Poly policy, I have total rights to any and all IP generated from this senior project. The purpose of this project is to evaluate whether a new class of polymers would be infeasible for improving the properties of fiber reinforced polymers produced by certain types of additive manufacturing. The deliverable will primarily be this report, which ideally will be instructive for elaborating on the invention I'm going to patent. Any connections that could exist between myself and external companies is not relevant within the scope of this senior project.

1.2 Broader impacts

Additive manufacturing refers to any manufacturing technique in which material is added to form a part as opposed to processes that begin with a block of material larger than the part volume and remove excess material. Additive manufacturing has been touted as a game-changing technology

that will revolutionize production at a global scale. [CITATION] Some proponents have gone so far as to say that this will represent a "democratization" of manufacturing, in which the up front costs are so low, anyone could start building useful parts for themselves or as a business.

However, the market data and predictions tell a different tale. Additive manufacturing and the raw materials used therein currently represent a XXXX dollar global market. [CITATION] While rapid growth is expected, bringing the value to XXXX by YYYYY, this is still a small fraction of the $10 trillion global manufacturing output, where single manufacturing technologies such as injection molding or machining are each worth hundreds of billions. [CITATION] This disparity is particularly noteworthy when it is considered that additive manufacturing encompasses multiple technologies each with completely different applications.

The details of each additive manufacturing process is beyond the scope of this project and several excellent reviews already exist in this area. [3] [4] [MORE CITATIONS] Instead a high-level overview will be given of a few classes of processes viewed from a materials perspective that considers their current commercial success and anticipated growth. Structural performance combined with scalability has been the primary factor affecting process viability in comparison to traditional manufacturing methods, thus functionally graded materials or finished parts that incorporate multiple components such as circuitry will not be considered.

Metals are the first important class of additive manufacturing materials and they typically involve powder processing. Metals have the obvious advantage over polymers of superior mechanical properties such as strength, stiffness, and durability. The additional benefit all additive manufacturing process posses has allowed metal additive manufacturing to find applications in a handful of high performance applications such as [LIST EXAMPLES]. Nevertheless, the exceedingly high cost of a metal additive manufacturing machine means scaling with parallel processing is not feasible for larger production runs and the applications will remain limited. [5]

In general, additive manufacturing processes are slow and therefore the only way to increase throughput at a reasonable cost is through parallel processing, unlike in traditional manufacturing where there is typically a focus on reducing time per part in a serial process. [CITATION? or self-evident] This brings us to the main polymer additive manufacturing processes. Polymer processes might have an even higher barrier to entry into final part commercial applications (as opposed to prototyping or mold-production) than metals since they fail to offer a significant and unique performance advantage in most commercial applications given their relatively poor mechanical properties. However, polymer based additive manufacturing processes lend themselves to far lower cost machines so wherever an innovation occurs in polymer processing that creates a novel commercial application, there is a far greater chance that parallel(y) scaling the process would be cost-effective. There are fields of innovations in polymer additive manufacturing that might enable this scalability: speed and performance.

Most polymer additive manufacturing processes are not competitive with injection molding for nearly any part, but faster printing can make it viable. Carbon3D is a company that has increased the speed of a polymer printing process[1] sevenfold and in doing so will find many parts that then make more sense to additively manufacture than injection mold, and their initial automotive industry partners prove this [CITATIONS].

Higher performance additive manufacturing with polymers could also enable serious applications and the clear path to achieve this is with carbon fiber reinforcement. Fiber reinforcement is available for selective laser sintering and fused deposition modeling (FDM), but the mechanical properties are typically not much higher than double that of the neat polymer. In comparison, carbon fiber composites with traditional manufacturing methods are usually more than an order of magnitude stronger and stiffer than the neat polymer. The reason for this disparity is that additive manufacturing methods are limited to using fibers shorter than the critical length due to processing constraints. This project will explore possibilities for narrowing this gap with longer fibers for fused deposition modeling, therefore possibly furthering global opportunities in additive manufacturing.

2 Literature review

This review will be broken up into three parts. The first will go over the general processing principles that control the subsequent structure in terms of length distribution of reinforcement fibers since polymer processing fractures discontinuous fibers causing a reduction in length. The second section will go over the micromechanics of short fiber composites and provide the motivation for fiber length preservation, as well as briefly summarizing existing data. The final section will provide an extension to the analytical techniques of the first section and go over fiber length characterization methods. After reading the literature review, the motivation for the following two questions that this research project seeks to address will become apparent.

- Does reduced viscosity in the post-compression section of extrusion decrease fiber length attrition?
- If so, is the reduction enough to have a ”substantial” effect on the material properties?

[1] Carbon3D does steriolithography, which uses a pool of resin that is pulled from an upside-down platform that UV cures the polymer as it is lifted.

2.1 Processing and structure

2.1.1 INJECTION MOLDING AND FILAMENT EXTRUSION PROCESS OVERVIEW

The literature on additive manufacturing filaments for FDM is fairly limited, but it is a fairly similar process to injection molding so we will integrate what is known from injection molding to guide this research. The injection molding process is fairly straightforward [Figure 2] [1]. In the first step, thermoplastic pellets are being fed by the hopper into the screw mechanism. Modern injection molding machines use shear forces within the screw rather than direct conductive heating to generate roughly 80% of the heat. Once a melt pool forms in front of the screw-tip, it plunges forward. In comparison, a filament extruder does not plunge forward and since the filament feeds at a slower continuous rate, the screw mechanism is sufficient to move the material forward. Both processes involve screw extrusion and are sometimes used with fiber reinforcement.

2.1.2 FIBER LENGTH ATTRITION MECHANISMS IN FILAMENT EXTRUSION

Fiber length attrition is caused by multiple factors and occurs in a few stages [Figure 1]. First, the initial crushing of the pellets begins the fiber breaking process. This pellet crushing is the primary heating process in an injection molding machine or filament extruder since they operate on the same principles. Once the fibers are in the melt-flow, they can be further broken by fiber-fiber, fiber-wall, or fiber-melt interactions [6] . Of these, it may be that the last one is most significant. When a fiber is in a melt flow it will not always be perfectly aligned with the flow. This misalignment allows the viscous shear forces from the fluid to inflict a stress on the fiber, which can surpass the fiber strength and cause fracture. The fiber stress that results in buckling by shear-induced axial compression has a critical value $(\eta\gamma)_crit$ for rodlike particles and it can be given as a function of shear rate and viscosity of the suspending medium Equation (1) [7].

$$(\eta\gamma) \approx \frac{E_b(ln(2a) - 1.75)}{2a^4} \tag{1}$$

where

η is shear rate

γ is viscosity

E_b is modulus of rupture

a is aspect ratio (l/d)

While this equation has been tested experimentally and could even be an exact representation for compression buckling, it neglects the bending of fibers [7]. When one considers bending, the fracture point is simply determined by thin rod theory [7] (2). Complex bending of fibers in suspension will in turn have an effect on the viscosity and it becomes difficult to model even if bending rather than buckling is the main source of fiber length attrition. Therefore, it is uncertain how much of a benefit can be obtained by changing processing parameters to reduce shear rate or changing the material to reduce intrinsic viscosity of the polymer.

$$R_{break} = \frac{Ed}{2\sigma_{fu}} \tag{2}$$

where

R_{break} is radius at which the rod breaks

d is fiber diameter

E is Young modulus

σ_{fu} is ultimate tensile strength of fiber

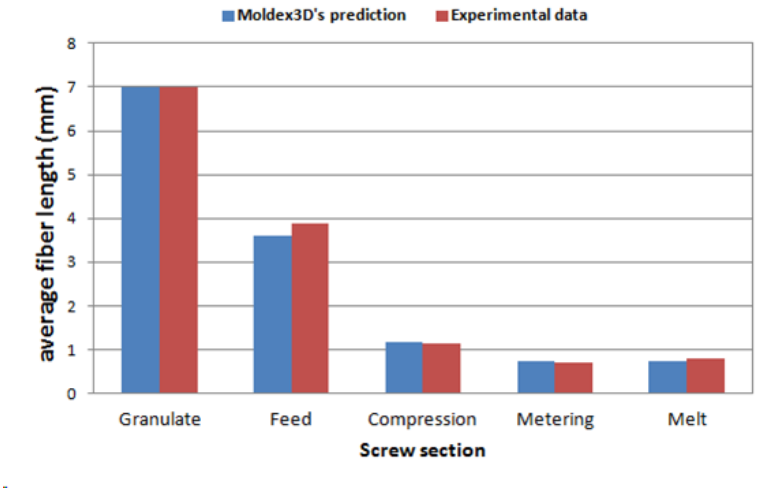

Figure 1 – Fiber length in different stages of injection molding.

2.1.3 Fiber length preservation

Since injection molding is 4 orders of magnitude higher throughput in the plunging step, design changes to screw shape with intent to make filament could be effective in reducing shear with current material systems. Studies have shown that screw geometry has an impact on fiber length

attrition, but since screw-extruders might not be re-designed for the filament extrusion process at lower shear rates, their could be some trivial optimization to be made that would result in substantial improvements [8].

Replacing thermoplastics with reversible-thermosets could be even more effective based on the previously mentioned critical buckling value since they quickly drop in viscosity. The company Evonik makes such a material. Their hybrid polymer thermosets, but then exhibits repeatable heat-induced de-crosslinking so it has the processability benefits of thermoplastics and thermosets. In the melt phase, the viscosity can be tailored and while not publicly disclosed, could be as low as typical thermosetting resins such as epoxies. Whether this is valuable for reinforced FDM filaments could be simulated with a low viscosity suspension of fibers to observe breakage. This would simulate only a portion of the process where the fibers break however, and it does not guarantee the material is a good option, but if it exhibits a large degree of fiber breaking it could rule it out. Furthermore, as the prior equations showed, the exact relation between viscosity and overall fiber attrition is unknown.

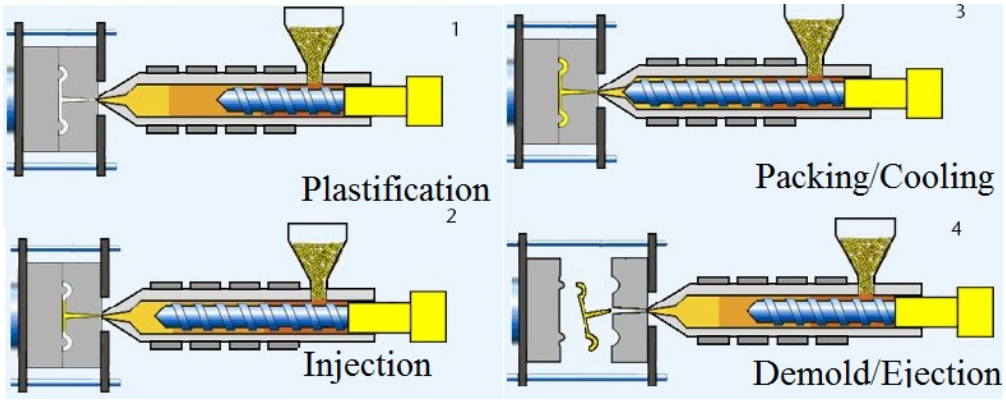

Figure 2 – A simplified view of the injection molding process [1].

2.2 Properties and performance

2.2.1 Performance of chopped fiber reinforcement

Chopped carbon fibers can be used in injection molded and FDM parts, but these parts are not nearly as strong as continuous fiber reinforced thermoplastics [9]. The strength of short fiber composites for a given composition is controlled by the length of the fibers and the interfacial adhesion between the fibers and the matrix. Higher adhesion and length means a larger area in which tensile loads can be transferred from matrix to fiber via shear loads, and the length of fiber at which the load transfer is sufficient to pull apart the fiber at failure rather than the fiber pulling out of the

matrix is defined as the critical length (Equation 3). This yields two cases with composite tensile strengths that can be modeled with the rule of mixtures [2] either the fibers are below the critical length (Equation 4) or they are above the critical length and will fracture (Equation 5).

$$l_c = \frac{\sigma_{fu} \cdot r}{\tau_i} \rightarrow \tau_i = \frac{\sigma_{fu} \cdot r}{l_c} \tag{3}$$

$$\sigma_{Ltu} = \tau_i \frac{l_f}{2 \cdot r} v_f + \sigma_{mu}(1 - v_f) \rightarrow \sigma_{Ltu} = \frac{\sigma_{fu}}{2} \frac{l_f}{l_c} v_f + \sigma_{mu}(1 - v_f), \qquad (l_f < l_c) \tag{4}$$

$$\sigma_{Ltu} = \sigma_{fu} \left(1 - \frac{l_c}{2 l_f}\right) v_f + \sigma'_m(1 - v_f), \qquad (l_f > l_c) \tag{5}$$

where

l_f is fiber length

l_c is critical length

σ_{fu} is ultimate fiber tensile strength

r is fiber radius

τ_i is interfacial shear strength (IFSS)

σ_{Ltu} is composite unidirectional ultimate tensile strength

v_f is fiber volume fraction

σ_{mu} is matrix ultimate tensile strength

σ'_m is matrix stress at fiber failure strain

These equation show that even if the fiber lengths are all at the critical length, the composite will still only reach half the strength of a continuous fiber composite (ignoring matrix contribution to strength). Specifically, when $l_c = l_f$, $\sigma_{ltu} = \frac{\sigma_{fu} v_f}{2} + \sigma_{mu}(1 - v_f)$. Below the critical length, the strength from the fibers is proportional to their length and to achieve comparable strength to continuous composites, the fiber lengths must be a few times longer than the critical length so

[2] These equations make various assumptions such as uniformity of shear stress along fiber and perfect matrix plasticity during failure among other. [10] These assumptions are of course false, but in trying to form a better model one runs into the problem that "[a] general theory of composite strength for an arbitrary fiber length and orientation distribution and local fiber density distribution for a part which is loaded in multiaxial stress does not exist." [11]. However, since this project merely attempts to experimentally prove a trend, this simple model should suffice.

that the fiber end effects become negligible, at which point the static[3] properties begin to plateau. Having a distribution of fiber lengths where many fibers are several times longer than the critical length can be achieved in two ways: 1) decrease the fiber length attrition during processing 2) improve the fiber matrix bonding to decrease the critical length. This project focuses on the former method, but since there is a wide variability in fiber matrix bonding even for the same constituent materials, we will provide an overview of typical values so that our experimental results can be considered in context.

2.2.2 Fiber matrix interface properties

Equation (3) showed that the critical length for a fiber of some diameter and strength is based solely on the the interfacial shear strength (IFSS). As IFSS increases there is a (decreasing) decrease in the critical length [Figure 3]. In practice, it is the critical length that is observed directly in experimentation via single fiber tests that measure residual fiber lengths, which then determine the IFSS since the relationship of Equation (3) is invertable.

IFSS can be thought of as a measure of how well the fiber bonds to the matrix. In general, fiber-matrix bonding can comprise covalent bonding, intermolecular bonding, and mechanical interlocking [probably should cite]. An interphase of nonzero thickness exists at the interface and the modulus of the interphase is an effective proxy for IFSS [probably should cite]. This is mentioned to make more obvious why it is not merely the matrix material and the fiber surface that determine IFSS, but also the processing parameters. Variations in crystallization based on cooling rates[4] as well as the residual stress due to the greater thermal expansion of polymer than fiber result in variations in IFSS for any given materials system. Studies with carbon fiber an PEEK have shown variations on the order of 1.5X for IFSS and 3X for interlaminar shear strength (ILSS) [12] [13].

ILSS is often easier to obtain than IFSS since it can be measured with bulk coupon tests rather than requiring specialized equipment to deal with individual fibers. IFSS and ILSS are sometimes used interchangeably, but they do not always correlate, and many studies only measure one property[5]. However, there exists a good review that covers various surface treatments and includes both ILSS and IFSS for various systems [14]. Furthermore, a table of ILSS values is provided (Table 1). Assuming IFSS values would be similar, this shows a typical range of critical lengths of about 300 μm to 500 μm, which suggests fiber lengths on the order of 2 mm would be sufficient to obtain high performance parts.

[3] Dynamic properties such as fatigue and creep might still be substantially worse than with continuous fibers.

[4] Elongational flows in additive manufacturing could plausibly also influence crystallization.

[5] The degree of correlation may relate to the relative values of the interface and bulk since one may operate as a limiting factor that gives artificially low experimental values due to the opposing failure mode taking place.

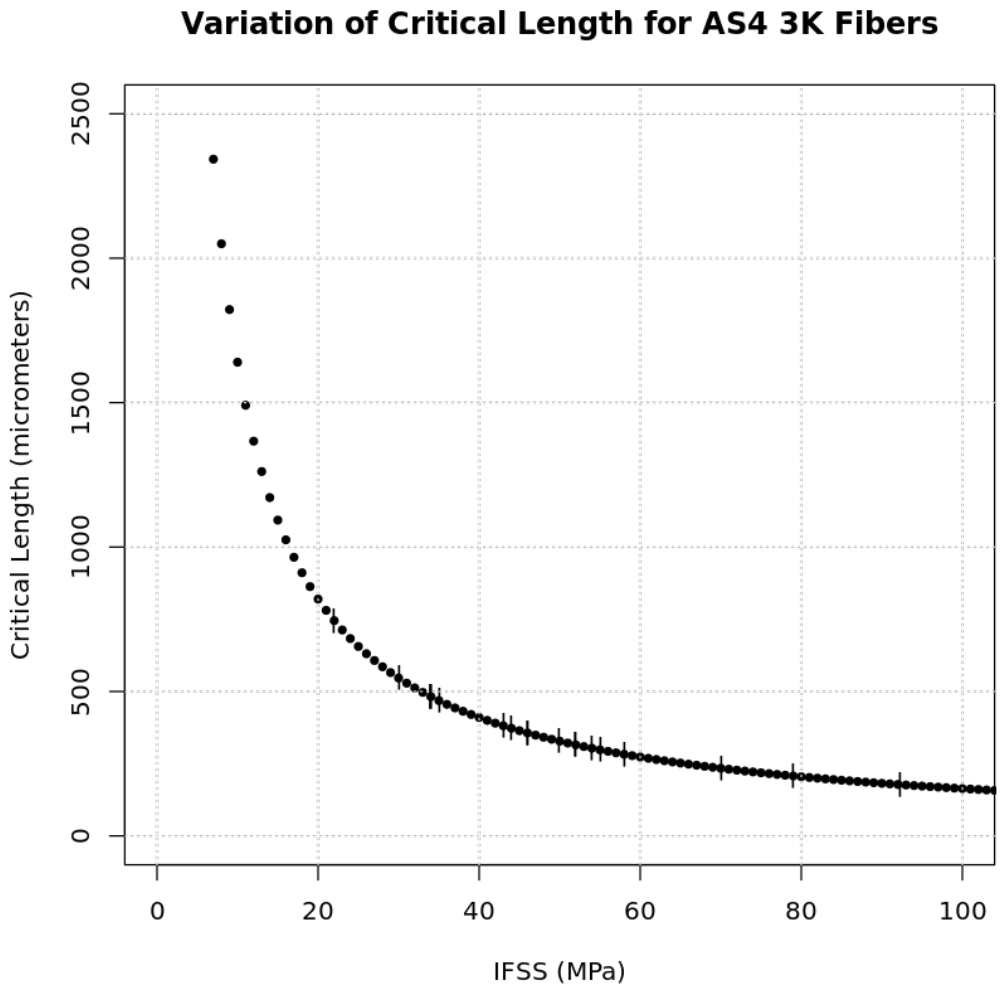

Figure 3 – Critical length shown as a function of interfacial shear stress. Ticks are values from Table 1.

2.3 Analysis and characterization

2.3.1 Non-point-mass length distribution

The equations of section 2.2.1 consider the variable of fiber length to be a single value, but since fiber attrition occurs, the lengths will not be constant. If one considers some discrete distribution of fiber lengths then one can use the same equations, although equations 3 and 4 must be combined since the distribution typically has fibers both above and below the critical length, and all constants can be removed from the summation (Equation 7). Constants are introduced to represent the volume fraction of subcritical and supercrical fiber lengths (Equations 8. Note that when v_f appears within a sum it means the volume fraction of the individual fiber in each term.

Treatment	Matrix	ILSS pre-treatment	ILSS post-treatment	Ref. and year
NO Plasma	PEEK	34	52	[15] 2011
NO Plasma	PES	30	46	[15] 2011
NO Plasma	PES	43	46	[15] 2011
Plasma	PC	22	44	[16] 2005
Plasma	PPESK[6]	70	79	[17] 2007
HNO_3	PEI	34	58	[18] 2011
γ-radiation	PEI	34	54	[19] [20] 2011
Nano YbF_3	PEI	34	52	[21] [22] 2011/2012
O_3	PA6	35*	55*	[23] 2008
MWNT, CVD	PMMA	12.5*	15.8*	[2] 2014
C_2H_4 + NH_3	PEEK	49.9*	92.2*	[24] 2012

Table 1: Summary of interface properties and corresponding critical lengths for various for various thermoplastic material systems and surface treatments [2]. Asterisks mean IFSS instead of ILSS.

The sum for supercritical fibers can be replaced with constants since the fibers have "full strength" minus the reduction near the ends. Therefore one merely needs to subtract this value from each fiber to determine the overall strength contribution. For subcritical fibers one notices that the product $v_F l_f$ comprises proportional terms and thus the strength contribution of a subcritical fiber is proportional to the square of its length. Both of these simplifications can be seen in Equation 7.

The reader might notice that σ' no longer appears in these equations. This is because the failure strain is not know a priori and thus the contribution of strength from the matrix has a larger estimate. The inaccuracy from this is much smaller than the bias from assuming the rule of mixtures model applies. One might also remove this term entirely.

$$\sigma_{Ltu} = \sigma_{fu}\left(\xi \sum_{l_f<l_c} \frac{v_f l_f}{2l_c} + \chi \sum_{l_f>l_c} v_f\left(1-\frac{l_c}{2l_f}\right)\right) + \sigma_m(1-v_f) \tag{6}$$

$$\sigma_{Ltu} = \sigma_{fu} v_f\left[\frac{\xi}{2l_c}\bar{S} + \chi\left(1-\frac{l_c}{2}N\right)\right] + \sigma_m(1-v_f) \tag{7}$$

$$\xi = \frac{\sum_{l_f<l_c} l_f}{\sum_{l_f<l_c} l_f + \sum_{l_f>l_c} l_f}, \quad \chi = 1-\xi \tag{8}$$

where

$\bar{S}$ is the average of the square of lengths of subcritical fibers

N is the number of supercritical fibers

ξ is the weight fraction of subcritical fibers

χ is the weight fraction of supercritical fibers

While most researchers report number or weight averages of fiber length distributions, these values are only useful for relative comparisons within a particular system of study since they do not map to any material property. Not only are these relative values not proportionally meaningful, it is possible for the property value of the model to move in the opposite direction of that suggested by the change in a length average due to strength plateauing at high values![7] Therefore, a reasonable person would seek a universal metric with the least deviation from linearity that has minimal dependence on the properties of the constituent materials. However, the non-linearities are dependent on the critical length so an ideal point metric does not exist, but one can define a function that provides the relevant metric for any particular critical length, thereby allowing universal comparisons among various studies and material systems (Equation 9)[8]. Analogous integral forms of these equations can also be constructed for theoretical consideration, but are of little practical value when working with actual data.

$$C : (\rho, l_c) \rightarrow [0,1] \qquad \text{by} \qquad C(\rho, l_c) = \frac{\xi}{2l_c}\bar{S} + \chi\left(1 - \frac{l_c}{2}N\right) \tag{9}$$

2.3.2 METHODS OF DETERMINING FIBER LENGTH DISTRIBUTIONS

The distribution of fiber lengths can be obtained by several methods. Sieves can be used, which allows histogram-like data to be obtained, but this method is considered unreliable since it can lead to fiber breakage, which skews the results. Another method that is beneficial when the fibers are in a solid matrix is scanning with X-ray microtomography. The preferred method involves obtaining a micrograph of a representative sample of fibers where the degree of overlap between fibers is little enough to allow some piece of software to effectively determine the length of each fiber and thus the length distribution of the sample. One researcher has suggested that 600 to 800 fibers is a representative sample, but the actual sample size needed would of course be dependent on the shape of the population distribution. While fiber length distributions are well modeled by Weibull distributions, the Weibull modulus and scale parameters are likely a function of the degree of fiber attrition, and the researcher should consider this in their analysis. If the fibers are embedded in

[7] Such a contrived scenario is unlikely to occur by a single attritive processing step. Consider half the fibers by weight at the critical length and the other half 100x critical length (50.5x is average) vs. all fibers 50x to see that it is possible.

[8] Fixing a fiber length distribution makes this a single variable function.

a matrix, the matrix can be dissolved, or preferably removed by pyrolysis in order to facilitate imaging.

3 Experimental procedures

3.1 Materials and overview of procedures

This research project aimed to experimentally determine the effect of the melt-flow portion of a single-screw-extrusion process on carbon fiber length attrition in isolation from the immediately preceding screw-plastication step that is responsible for most of the heat needed for melting with current screw-based designs. It was determined that using silicone oil of various fixed viscosities could be used to simulate the melt-flow portion of extrusion in complete isolation of the pellet-crushing plastication step that is required. A summary of the steps carried out is provided followed by a detailed description of each step.

1. Chopped carbon fibers with an initial length of 2.0 mm were heated in an oven 150^{o}C for 2 hours to break up the fascicular structure that is held together by water.
2. Ten percent carbon fiber by volume was added to two samples of silicone oil with viscosities of 5,000 and 10,000 centipoise (20k–35k (cP) are typical values).
3. Both suspensions were passed through a hobbyist style additive manufacturing filament extruder, with a 3.0 mm final diameter tapered die.
4. The extrudates where placed in a container of mineral spirits for 24 hours to allow the silicone oil to dissolve, and then vacuum filftered to separate the carbon fibers.
5. The carbon fibers were dispersed in water with the use of heat and an ultrasonication bath. A small amount of the suspension was poured into a shallow glass container and slowly heated, leaving a layer of fibers.
6. The fibers were photographed, but the fiber length distribution was only obtained for the 10,000 cP sample.

3.2 Sample Preparation

Chopped carbon fibers with a constant length of 2 mm were obtained from [COMPANY]. These chopped carbon fibers are cut from a 3K tow of carbon fiber and each fasicular bundle is held together with approximately 15% humidity by weight. This humidity holds together the bundle of fibers and prevents damage during handling, which ensures all the fibers maintain their initial

length. Chopped carbon fibers were placed in a 600 mL beaker and placed in an oven at 150 ^{o}C for about two hours. The temperature should be low enough to avoid fiber damage via oxidation, which does not occur below [TEMPERATURE]. Therefore, the sample needs to be heated until all the individual fiber bundles have fallen apart [Figure 4][Figure 5] [FIGURE, undried on one side, mostly dried on the other]. It should be noted that if the sample is left unattended for an extended period of time, it may be necessary to heat the fibers again.

Figure 4 – Carbon fibers as received in fascicular bundles prior to drying.

Figure 5 – Carbon fibers that are nearly dried with a few bundles remaining.

Once the fibers were dried, samples were weighed on an enclosed scale. It should be noted that the fibers have a propensity to become airborne once dried and all sample manipulations should be done in a fume hood or with adequate respiration equipment. The silicone oil was weighed and the carbon fiber stirred into the silicone oil with a glass stir rod. Since the relative density of the carbon fiber decreases when it is poured, the carbon fiber had to be gradually mixed in [Figure 6]. About 4 ounces of each sample were prepared.

Figure 6 – Prepared samples of carbon fibers in silicone oil.

3.3 Sample Processing

3.3.1 Extrusion

A filastruder is a single screw extruder meant for producing filament for 3D printing [Figure 7. Each sample was fed through the Filastruder with no heat, and a modified nozzle with a taper ending a 3 mm diameter die. The diameter and tapering was selected due to preliminary experiments which showed jamming with smaller sizes. Furthermore, a 500 and 1,000 cP sample had also been prepared in preliminary tests and experienced similar jamming. However, these samples with the lowest viscosity failed by separation where the oil would be pressed out of the extruder without carbon suggesting that their is a minimum viscosity necessary to ”drag-along” the fibers through a constriction for any given set of processing and materials parameters.

3.3.2 Fiber-oil separation

Once the two samples had been passed through the extruder it was necessary to obtain a planar image of the fibers in order to obtain their length distribution. A sample far smaller than a cubic centimeter was placed in a beaker with a few ounces of mineral spirits, which almost entirely dissolved the silicone oil within 24 hours as evidenced by thorough dispersion of the fibers in the mineral spirits. Mild agglomeration in these samples occurred, which was readily overcome with a few seconds of ultrasonication in a bath of water. The fibers were removed from the mineral spirits via vaccuum filtration [Figure 8]. It seemed that the dissolved silicone oil was not easily passing through the filter since the 2 ounce samples required about 24 hours to pass through the filter.

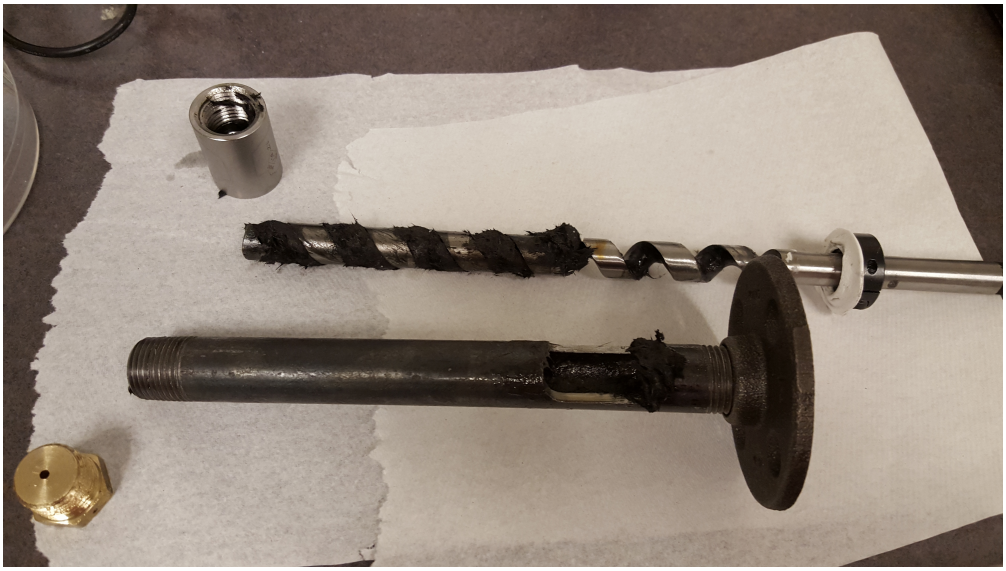

Figure 7 – Screw and chamber of the Filastruder with carbon fiber and oil during preliminary tests.

Figure 8 – Vacuum filtration process with ultrasonication bath in background on the left.

3.3.3 Fiber isolation and imaging

individual fibers were then placed in beakers with de-ionized water. Initial attempts to re-disperse fibers that were agglomerated, presumably from residual silicone oil, failed even after 10 minutes in an ultrasonication bath. A small amount of heat from a hot plate below the boiling point of water, interspersed with ultrasonication was finally effective in dispersing the fibers. Then a sample of the fibers in solution were poured into a shallow glass dish such that the amount of fibers was

maximized with the constraint that there be minimal fiber overlap in the horizontal plane. Heating these dishes on a hot plate evaporated the water, leaving a layer of carbon fibers. Initial observation of the fibers under a microscope showed that the fibers were too long to capture a sufficient number of fibers within the field of view of the microscope even on the lowest magnification setting of 5X. Therefore, images of the dishes with fibers were taken in a room lit by sunlight with a blank sheet of paper underneath.

3.4 Data Analysis Methods

The fibers appeared very faint in the initial images and it would have been difficult to pin down the endpoints [Figure 9]. Enhancing the contrast with standard image tools was ineffective. Therefore, a Python script was used to improve the visibility of the fibers that were previously very faint [Figure 10]. The script makes pixels below a cutoff value switch to black within a grid location, for all grid locations. It is necessary to have a grid in place due to the overall brightness gradient. A modified Matlab script was used to manually extract endpoint positions by clicking on the endpoints [Figure 11]. Then the endpoints were converted into lengths and graphed in R.

Figure 9 – Original image of fibers in glass dish.

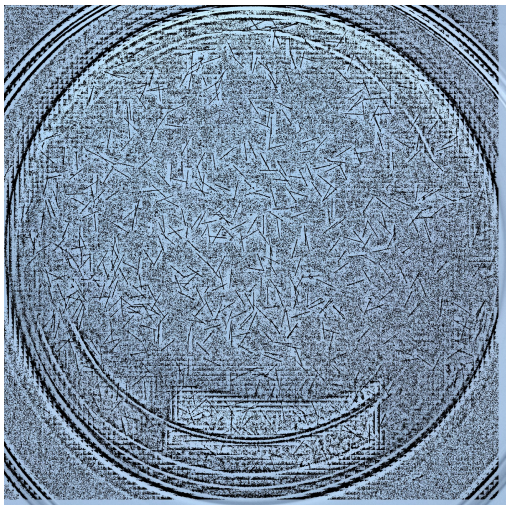

Figure 10 – Image of fibers after running image through Python script.

```
from PIL import Image
from PIL import ImageFilter
import math
image = Image.open("fin.JPG")
image = image.filter(ImageFilter.SMOOTH)
width = image.size[0]
height = image.size[1]
pixels = image.load()
xMesh = 100
yMesh = 100
threshold = .9
meshWidth = width / xMesh
meshHeight = height / yMesh
for x in range(xMesh):
  for y in range(yMesh):
    xStart = x * meshWidth
    yStart = y * meshHeight
    xFinish = xStart + meshWidth
    yFinish = yStart + meshHeight
    brightness = []
    for i in range(xStart, xFinish):
      for j in range(yStart, yFinish):
        p = pixels[i, j]
        brightness = brightness + [p[0] + p[1] + p[2]]
        avg = sum(brightness)/len(brightness)
        low = min(brightness)
        high = max(brightness)
        gap = float(avg - low)
        floor = low + threshold * gap
        counter = 0
    for i in range(xStart, xFinish):
      for j in range(yStart, yFinish):
        if brightness[counter] < floor:
          pixels[i, j] = (0, 0, 0)
        counter += 1
image.save("fout.JPG")
```

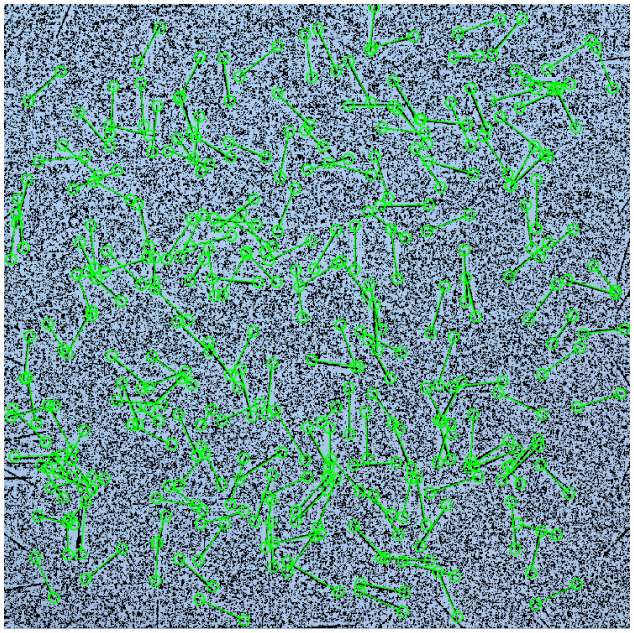

Figure 11 – Selection from transformed image with green lines showing each segment that was selected in Matlab.

4 Results and Discussion

4.1 Resulting fiber length distribution

The length distribution of the sample had a peak centered just below the initial length of 2 mm, but a spread that went above 2 mm [Figure 12]. There was no ”carbon dust” in the sample, nor where there any fibers below 0.5 mm, which means there could not be any fibers in the 1.5 mm to 2.0 mm range as these data suggest. Therefore, it must be that virtually all these fibers were exactly their initial length of 2 mm except for the very few fibers that fractured in half. The noise in the image and imprecision and inaccuracy of clicking on endpoints shows the drawbacks of this method in comparison to sophisticated software that determines the exact endpoints of each fiber. It was apparent that the same data would result from the 5,000 cP sample, so the fiber lengths from that sample were not obtained.

4.2 Implications

This project demonstrates that at shear rates used to extrude filament for additive manufacturing, the viscosity is inconsequential to attrition during the melt-flow. Average fiber lengths in thermoplastics often drop to about 0.2 mm, or an order of magnitude lower than what was observed in this study.

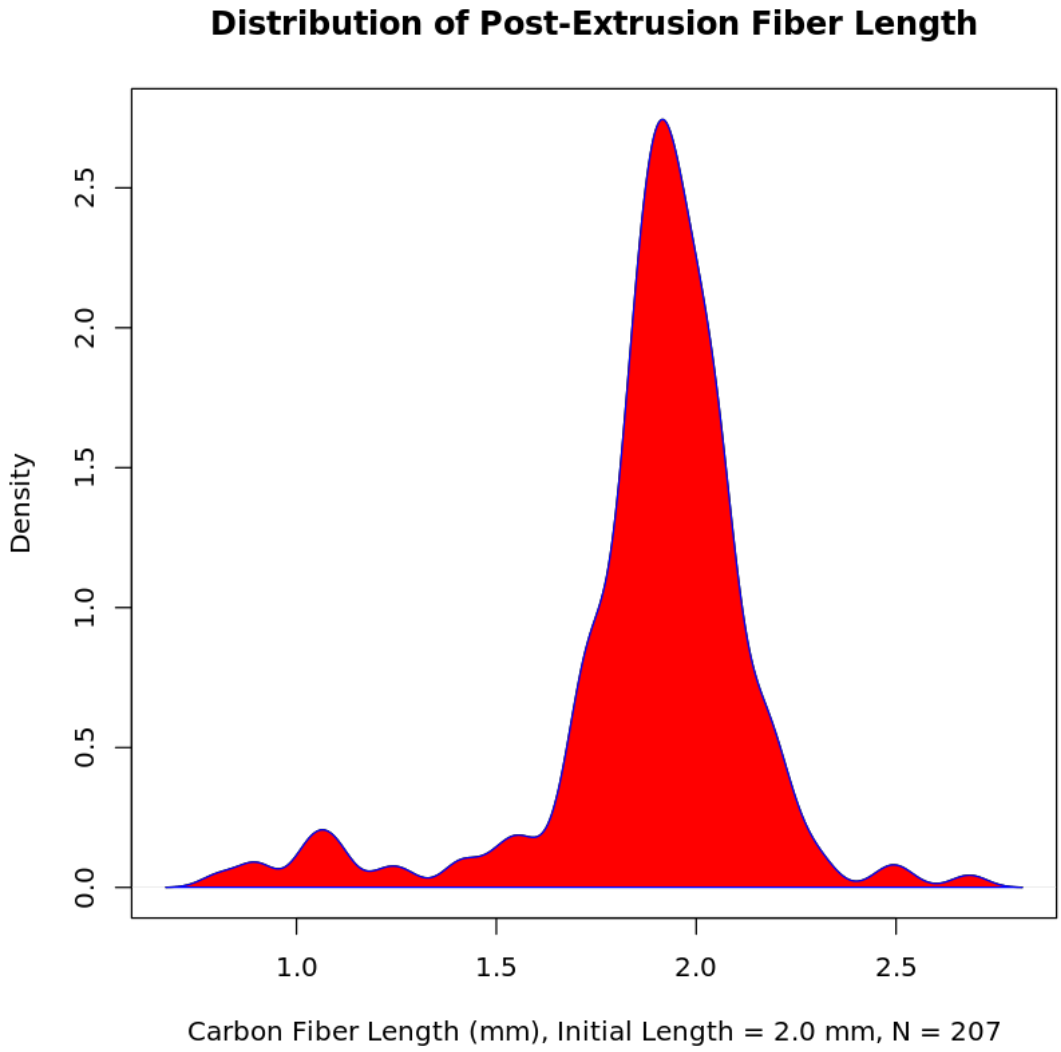

Figure 12 – Distribution of fiber lengths.

This means the melt-flow process does not impose a limiting factor that might otherwise make the fiber lengths end up far below typical critical lengths despite other processing conditions. This can be concluded since 10,000 cP is only a third to a half the viscosity of a typical thermoplastic during processing, and the probability of fiber damage is proportional to the product of viscosity and shear rate. Injection molding operates at shear rates that are four orders of magnitude higher than filament production. Therefore, viscosity might still be a relevant factor for the melt-flow at those higher viscosities, and it could also have an effect on the fiber damage in the plastication step.

4.3 Further research

The most immediately applicable research going forward should focus on how to reduce damage from screw-plastication rather than decreasing viscosity to preserve fiber length. Irrespective of whether plastication damage can be reduced at lower viscosities, it would be beneficial to decrease the amount of plastication by using conductive, radiative and/or inductive heating in a piston-plunger style extruder to obtain higher performance materials [FIGURE plunger extrusion]. Given that it is 8 times easier to buckle a fiber twice as long, one could expect such a system to produce filaments with fibers greater than 1 mm in length. 1 mm fibers are double the critical length of a composite with a low interfacial shear strength of 30 MPa so it is reasonable to anticipate vastly improved performance and numerous new applications for additively manufactured parts that could be made with such materials.

5 Conclusion

A review of the motivations behind additive manufacturing and their current limitations was provided. A study was carried out to gain a greater understanding of the fiber length attrition in the process used to produce short fiber reinforced filament for FDM additive manufacturing. The results of the study unexpectedly showed that at the low strain rates used to produce such filament, plastication can be the only part of the process causing the bulk of the fiber length attrition. A method of producing filament that removed the plastication step that might produce vastly superior filament was presented. Furthermore, a novel method of determining fiber length distributions was shown to be viable in obtaining approximate data, with easier implementation than traditional methods.

6 References

[1] Lei Xie, Bingyan Jiang, and Longjiang Shen. Modelling and Simulation for Micro Injection Molding Process. INTECH Open Access Publisher, 2011. (document), 2.1.1, 2

[2] Mohit Sharma, Shanglin Gao, Edith Mäder, Himani Sharma, Leong Yew Wei, and Jayashree Bijwe. Carbon fiber surfaces and composite interphases. Composites Science and Technology, 102:35–50, 2014. (document), ??, 1

[3] Kaufui V Wong and Aldo Hernandez. A review of additive manufacturing. ISRN Mechanical Engineering, 2012, 2012. 1.2

[4] Samuel H Huang, Peng Liu, Abhiram Mokasdar, and Liang Hou. Additive manufacturing and its societal impact: a literature review. The International Journal of Advanced Manufacturing Technology, 67(5-8):1191–1203, 2013. 1.2

[5] William E Frazier. Metal additive manufacturing: A review. Journal of Materials Engineering and Performance, 23(6):1917–1928, 2014. 1.2

[6] HJ Wolf. Screw plasticating of discontinuous fiber filled thermoplastic: Mechanisms and prevention of fiber attrition. Polymer composites, 15(5):375–383, 1994. 2.1.2

[7] Anita Vaxman, Moshe Narkis, Arnon Siegmann, and Samuel Kenig. Short-fiber thermoplastics composites: Fiber fracture during melt processing. Wiley Encyclopedia of Composites, 2012. 2.1.2, 2.1.2

[8] Karthik Ramani, Dave Bank, and Nick Kraemer. Effect of screw design on fiber damage in extrusion compounding and composite properties. Polymer composites, 16(3):258–266, 1995. 2.1.3

[9] Weihong Zhong, Fan Li, Zuoguang Zhang, Lulu Song, and Zhimin Li. Short fiber reinforced composites for fused deposition modeling. Materials Science and Engineering: A, 301(2):125–130, 2001. 2.2.1

[10] Pankar K Mallick. Fiber-reinforced composites: materials, manufacturing, and design. CRC press, 2007. 2

[11] Robert C Wetherhold. Short-fiber-reinforced polymeric composites: Structure–property relations. Wiley Encyclopedia of Composites, 2012. 2

[12] Shang-Lin Gao and Jang-Kyo Kim. Crystallinity and interphase properties of carbon fibre/peek matrix composites. 2.2.2

[13] H Sugihara and FR Jones. Promoting the adhesion of high-performance polymer fibers using functional plasma polymer coatings. Polymer Composites, 30(3):318–327, 2009. 2.2.2

[14] Long-Gui Tang and John L Kardos. A review of methods for improving the interfacial adhesion between carbon fiber and polymer matrix. Polymer composites, 18(1):100–113, 1997. 2.2.2

[15] Sudhir Tiwari, Mohit Sharma, Stephane Panier, Brigitte Mutel, Peter Mitschang, and Jayashree Bijwe. Influence of cold remote nitrogen oxygen plasma treatment on carbon fabric and its composites with specialty polymers. Journal of Materials Science, 46(4):964–974, 2011. ??, ??, ??

[16] MA Montes-Morán, FWJ Van Hattum, JP Nunes, A Martinez-Alonso, JMD Tascón, and CA Bernardo. A study of the effect of plasma treatment on the interfacial properties of carbon fibre–thermoplastic composites. Carbon, 43(8):1795–1799, 2005. ??

[17] Chun Lu, Ping Chen, Qi Yu, Zhenfeng Ding, Zaiwen Lin, and Wei Li. Interfacial adhesion of plasma-treated carbon fiber/poly (phthalazinone ether sulfone ketone) composite. Journal of applied polymer science, 106(3):1733–1741, 2007. ??

[18] S Tiwari, J Bijwe, and S Panier. Tribological studies on polyetherimide composites based on carbon fabric with optimized oxidation treatment. Wear, 271(9):2252–2260, 2011. ??

[19] S Tiwari, J Bijwe, and S Panier. Gamma radiation treatment of carbon fabric to improve the fiber–matrix adhesion and tribo-performance of composites. Wear, 271(9):2184–2192, 2011. ??

[20] Sudhir Tiwari, J Bijwe, and S Panier. Polyetherimide composites with gamma irradiated carbon fabric: studies on abrasive wear. Wear, 270(9):688–694, 2011. ??

[21] Sudhir Tiwari, J Bijwe, and S Panier. Role of nano-ybf3-treated carbon fabric on improving abrasive wear performance of polyetherimide composites. Tribology Letters, 42(3):293–300, 2011. ??

[22] S Tiwari, J Bijwe, and S Panier. Enhancing the adhesive wear performance of polyetherimide composites through nano-particle treatment of the carbon fabric. Journal of Materials Science, 47(6):2891–2898, 2012. ??

[23] J Li. Interfacial studies on the o 3 modified carbon fiber-reinforced polyamide 6 composites. Applied surface science, 255(5):2822–2824, 2008. ??

[24] Anil N Netravali and Kashmiri L Mittal. Fiber surface treatment: relevance to interfacial characteristics. Wiley Encyclopedia of Composites, 2012. ??